TOWARD EFFECTIVE STRUCTURAL IDENTIFICATION OF MEDIUM-RISE BUILDING STRUCTURES

A. Nguyen, K.A.T.L Kodikara, T.H.T. Chan & D.P. Thambiratnam

School of Civil Engineering and Built Environment, Queensland University of Technology, Brisbane, Australia. Email: a68.nguyen@qut.edu.au

ABSTRACT

Structural Identification (St-Id) is the process of constructing and calibrating a physics-based model based on the measured static and/or dynamic response of the structure. Over the last two decades, although the St-Id methods have become increasingly popular amongst civil-structural engineering communities, most complete and successful applications are often found with flexible structures such as long-span bridges and towers. Very few comprehensive studies were reported on building structures, especially those with medium-rise characteristics which are often associated with complicated analytical modelling and different degrees of parameter uncertainties. To address this need, this paper presents an in-depth study on St-Id of a benchmark medium-rise building firstly demonstrating the importance of developing appropriate initial analytical models that can be used for the automated model calibration techniques. Then, a novel parametric study based sensitivity analysis approach is introduced to identify tuning parameters as well as their appropriate ranges to maximise the correlation of the calibrated model whilst preserving the physical relevance of the calibrated model. Modal data of the first few modes measured under ambient vibration conditions are used in this study.

KEYWORDS

Structural identification (St-Id), medium rise building, finite element modelling, automated model calibration, sensitivity analysis, modal data

1 Introduction

Structural identification (St-Id) can be defined as the system identification of civil structures by developing and calibrating a physics-based analytical model with the dynamic response of actual structures [1]. Although there are a number of definitions for St-Id process found in the literature, the main components of St-Id can hence be identified as (1) structural conceptualization and development of analytical models (2) identification of dynamic characteristics of the actual structure through experimental evaluations (3) model calibration and validation [1-3]. The application of St-Id was first in earthquake engineering to identify the dynamic characteristics of civil structures such as buildings, dams and nuclear facilities [4-6]. With the advancement in computer, sensor and testing technologies, during the last two decades, civil engineering researchers became interested in utilising vibration based St-Id for condition assessment and health monitoring of real constructed systems [7-11].

So far, finite element (FE) modelling has no doubt been the most popular approach to develop physics-based analytical models for real civil structures. However, even with the presence of the most sophisticated software packages, development of a complete and representative FE model is still a very challenging task [1]. Common uncertainties that are difficult to be completely eliminated in the FE modelling process are simplifying assumptions of geometrical and material properties of the structure and uncertain boundary conditions [12]. Hence, before using the analytical models for any further analysis tasks, it is important to properly correlate and calibrate the initially developed FE model by means of experimental data collected from the actual structure most dominantly in the form of modal data such as frequencies and mode shapes. In recent years, operational, or output-only, modal analysis (OMA) has usually been the preferred experimental approach, in comparison with the conventional input-output

counterpart, due to obvious benefits such as its economical aspect and better suitability for in-service structures.

Once the FE model is properly correlated with the experimental data, model calibration task can be conducted. Model calibration can be described as the process of correcting the modelling errors of an analytical FE model using measured data and this technique is applied to generate a refined baseline FE model that accurately predicts the dynamic or static behaviour of a structure. The purpose of model calibration is to adjust the mechanical and materials properties as well as geometrical properties of structural elements to obtain a better agreement between the developed physics-based FE model and experimental results. For civil engineering structures, the most popular model calibration methods are based on sensitivity analysis and often implemented in iterative computation manners [13]. These methods first identify the uncertain parameters through a comprehensive sensitivity analysis and systematically change the parameters to minimise the discrepancies between FE model and test data often conducted using an iterative procedure. Several successful case studies can be found in literature using automated sensitivity based model calibration methods predominantly in flexible structures such as footbridges, long-span highway bridges, bridge towers and tall buildings [13-20]. However, very few studies are reported on complete St-Id processes on buildings especially those with medium-rise characteristics [21]. These types of structures are often associated with complicated structural details leading to challenges for the users in developing satisfactory initial FE models for St-Id purposes. Further, the presence of different degrees of parameter uncertainties leads to difficulties in maintaining the tuning parameter variations in appropriate ranges during the model calibration process.

To address the above issue, this paper presents a comprehensive St-Id process of a reasonably complex medium-rise building structure with a focus on solutions to obtaining satisfactory initial FE models as well as appropriately controlling and managing the automated model

calibration process to overcome difficulties associated with this type of structure. The test structure is a landmark building of Queensland University of Technology (QUT) which was equipped with a long-term monitoring system to capture ambient vibration responses. The rest of this paper is presented as follows. Section 2 provides a brief description of the test structure as well as the relevant monitoring system and measured data. Strategies to obtain an appropriately representative FE model are then demonstrated in Section 3 while Section 4 gives detailed solutions for managing the complex model calibration process. Finally, Section 5 summarises the findings and recommendations from the research.

2 Test structure, monitoring system and measured data

The test structure considered in this paper is the main building, named P block, of the Science and Engineering Centre (SEC) at QUT's Gardens Point Campus in the city of Brisbane (Fig. *1*~~Fig. 1~~). Known as one of the most innovative and dynamic community hubs in the Southern Hemisphere, the SEC P block houses state-of-the-art analytical research instruments worth of A$17 million and a giant digital lab named "the Cube" (www.thecube.qut.edu.au) with 48 multi-touch high-definition screens soaring across two storeys amongst other modern scientific facilities. With its sustainable design, the SEC was awarded a 5-star Design Education V1 Certified rating by the Green Building Council of Australia making it one of the highest-rated 'green' buildings in Brisbane [22].

Fig. 1 P block building: front corner view (left) and side view with sensor positions (right)

Structurally, P block is a reinforced concrete (RC) frame structure with post tensioned slabs and RC columns. The building has four semi-underground levels the footprint of which are approximately 75m x 65m. The six upper floor levels have a smaller area with approximate dimensions of 65m x 45m. The total height of the building is 42m from the formation level of the building while the floor height of the building varies in the range 2.7m to 4.5m. Even though the structure has an overall rather common configuration, when concerning the structural detailing the building has many variations in terms of slab thicknesses, slab openings, column sizes and orientations. Three main shear walls are placed in the middle of the building, two to the east and other to the west to resist the lateral loads due to potential wind, lateral seismic loads and torsional forces. A level 4 layout which can be considered as a typical floor level is presented in Fig. 2~~Fig. 2~~.

Formatte

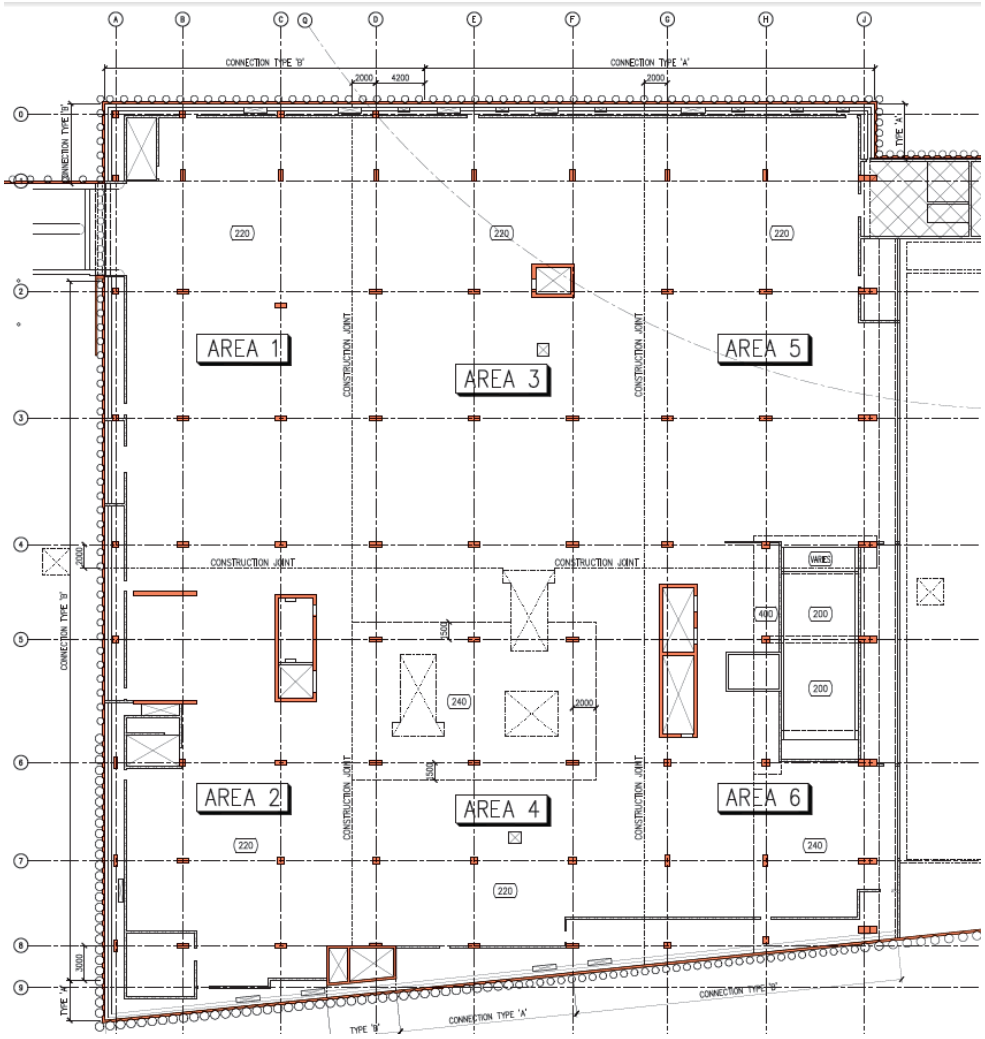

Fig. 2 Level 4 layout of P block

As an important public venue and ‘smart’ building, P block was well instrumented with three permanent monitoring subsystems [23], but for the scope of this paper only the vibration monitoring system and its measured data will be described further. At its peripheral level, the vibration monitoring system consists of six tri-axial accelerometers and two single-axis accelerometers all with +/-2g input range and 2V/g sensitivity. The sensors were located on levels 4, 6, 8 and 10 (see Fig. *1*~~Fig. *1*~~ right) aiming to acquire vibration responses in ambient excitation conditions to enable long-term assessment. Due to large measurement coverage of the monitoring systems herein, a distributed data acquisition (DAQ) system architecture was adopted and, for each DAQ node, a controller and chassis integrated system model cRIO-9074

was employed to power and control each sensor via an analog input module NI-9239. To synchronize multiple local sensor clusters, a TCP/IP command based data synchronization method was derived for use as a cost-effective replacement for the traditional hardware based synchronization schemes. Acceleration data was acquired continuously under ambient excitation conditions and split into 30 minute subsets for operational modal analysis (OMA) purposes. To deal with large number of datasets, the advanced OMA technique named data-driven stochastic subspace identification (SSI-data) was used to estimate modal information and up to six well-excited modes were estimated. Fig. 3~~Fig. 3~~ showed the building model used for SSI-data analyses and the animated shapes of the first five modes which will be used further in this paper. More detail of the P block system and previous SHM studies can be found in previous publications of the authors [23-25].

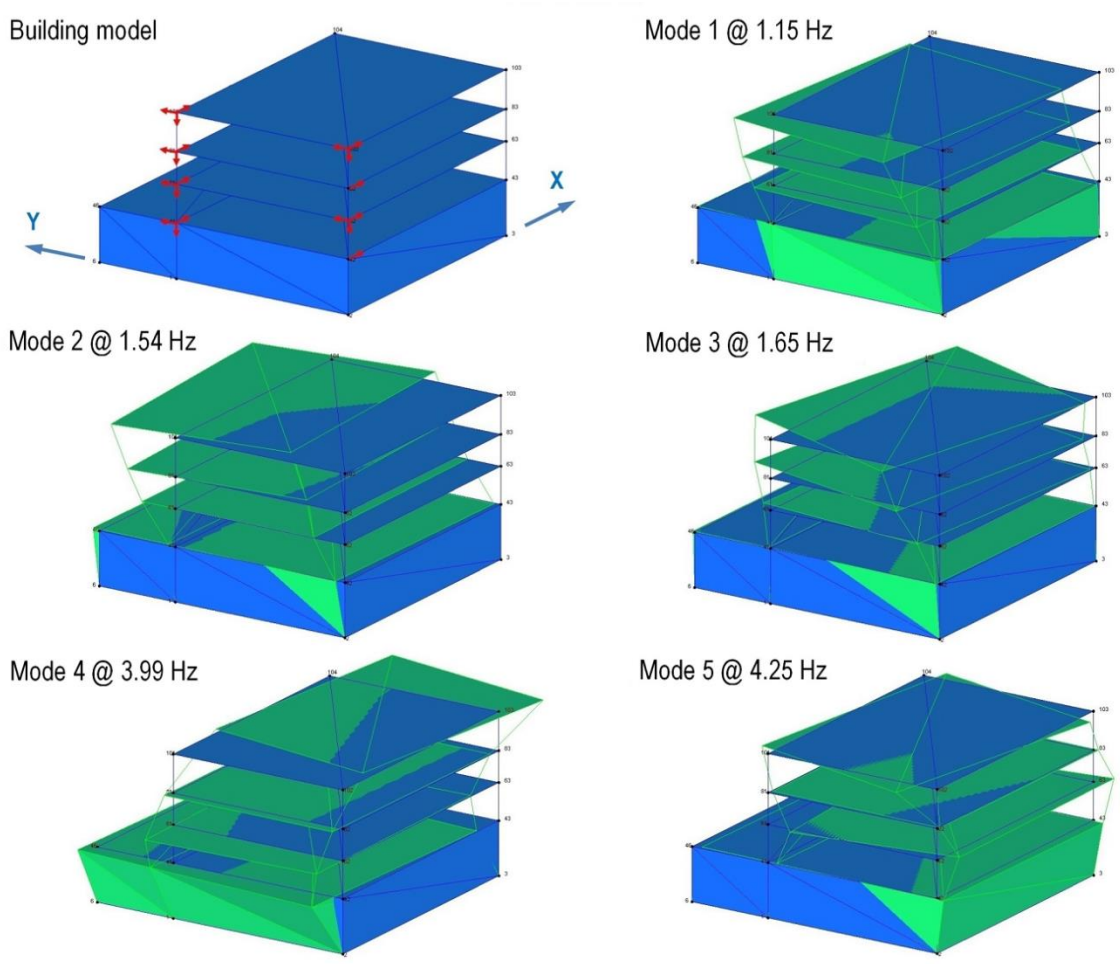

Fig. 3 Building model for OMA and typical animated shapes of first five vibration modes

3 Structural Conceptualization and Development of Analytical Models

It is important to understand the difference in structural conceptualization and development of analytical models at different engineering stages such as the design stage or post-construction stages so that an appropriate analytical model can be chosen. To study this phenomenon for the P block structure, the results of a simple FE model developed based on the design drawings were checked against the OMA data. The results were completely unsatisfactory as the original error for the frequencies of first three modes is close to 50% and the model calibration resulted in over 100% change to the selected parameters. Hence, more detailed FE models were developed based on the fixities of the four semi-underground basement walls using the commercially available software package SAP2000 of Computer and Structures, Inc. (www.csiamerica.com) to obtain the most suitable initial analytical model for the model calibration. The common considerations taken during the development of all three initial FE models are summarized below;

- To enable the torsional behaviour of the FE models to be as close as possible to the real structure, detailed modelling was considered when dealing the shear cores to take into account major and minor openings and internal thin walls
- To maintain the rigid behaviour of floor levels floor diaphragms were assigned to each floor level
- The spandrel beams were modelled as shell elements instead of commonly used frame elements
- The non-structural components (NSCs) were not included in the FE models; since the building cladding was fully glazed and all the partitions were light-weight initial investigations revealed that the effect of mass and stiffness of NSCs was negligible.

- Average slab thicknesses were considered in the FE models; since the building consists of complex interior slab configurations made it impossible to model the floor slabs in detail. This could be justified since in the automated model calibration floor slab thickness can be used as an uncertain parameter to account for the simplifying assumptions used in the initial FEM.

Based on these rules, three different initial models were developed based on different fixities of the four semi underground basement walls of the structure. In the first model (FE model 1) no fixities were considered in any basement walls, while second model (FE model 2) had fully fixed condition used in all four basement walls and the third model (FE model 3) employed fully fixed condition for all horizontal basement walls for the first two levels.

The natural frequencies and mode shapes obtained from the OMA and all three FE models were compared to identify the most appropriate analytical model for the automated model calibration. For mode shape correlation, modal assurance criterion (MAC) was used and the following equation was used to compute the MAC between an analytical (index a) and experimental mode shape (index e);

$$\left(MAC(\Psi_a, \Psi_e)\right) = \frac{\left|(\{\Psi_a\}^t\{\Psi_e\}\right|^2}{(\{\Psi_a\}^t\{\Psi_a\})(\{\Psi_e\}^t\{\Psi_e\})} \quad (1)$$

Comparison of the frequencies and mode shapes of OMA results with the three initial FE models are presented in Table 1~~Table 1~~ and Table 2~~Table 2~~ respectively. By analysing the correlation data of all three analytical models, it is clear that although FE model 3 has better correlation in terms of frequencies for some modes (modes 1, 2 and 4), FE model 1 has the overall best correlation in terms of frequencies and mode shapes of all five modes hence this model is chosen for the automated model calibration.

Formatte

The FE model 1, as shown in Fig. 4~~Fig. 4~~ consists of 1400 frame elements (to model all the columns) and 8000 shell elements (for slabs -5680 and shear walls -2320). As illustrated in Fig. 4~~Fig. 4~~ all of the first five modes are global, and in the range of 0.990 Hz to 4.972 Hz frequencies and detailed features of these modes are presented in Table 1~~Table 1~~. The largest frequency error is 16.88 % occurred at mode #5 while MAC values of FE model 1 against OMA data (Table 2~~Table 2~~) have below par values for some modes (e.g. #2 and #3), which can both be attributed to uncertainties from the large-scale structure modelling tasks as well as the demanding ambient vibration testing conditions.

Table 1 Comparison of frequencies of three different FE models against OMA results

Mode No	Description of Modes	Freq ^{OMA}	Freq ^{FEM} [Error $^{FEM\ vs.\ OMA}$]		
			FE model 1	FE model 2	FE model 3
1	1st translational – X direction	1.147 Hz	0.990 Hz [-13.69 %]	1.332 Hz [16.13 %]	1.010 Hz [-11.94 %]
2	1st translational – Y direction	1.544 Hz	1.452 Hz [-5.96 %]	1.717 Hz [11.20 %]	1.502 Hz [-2.72 %]
3	1st torsional	1.653 Hz	1.678 Hz [1.51 %]	1.987 Hz [20.21 %]	1.723 Hz [4.23 %]
4	2nd translational – X direction	3.989 Hz	3.680 Hz [-7.75 %]	4.746 Hz [18.98 %]	3.787 Hz [-5.06 %]
5	2nd torsional	4.254 Hz	4.972 Hz [16.88 %]	5.325 Hz [25.18 %]	5.111 Hz [20.15 %]

Table 2 Comparison of MAC values of three different FE models against OMA results

Mode No	MAC Values (vs. OMA)		
	FE model 1	FE model 2	FE model 3
1	89.9 %	80.3 %	88.9 %
2	50.5 %	11.1 %	36.9 %
3	42.5 %	12.8 %	35.0 %
4	63.2 %	52.5 %	59.2 %
5	68.4 %	30.2 %	59.7 %

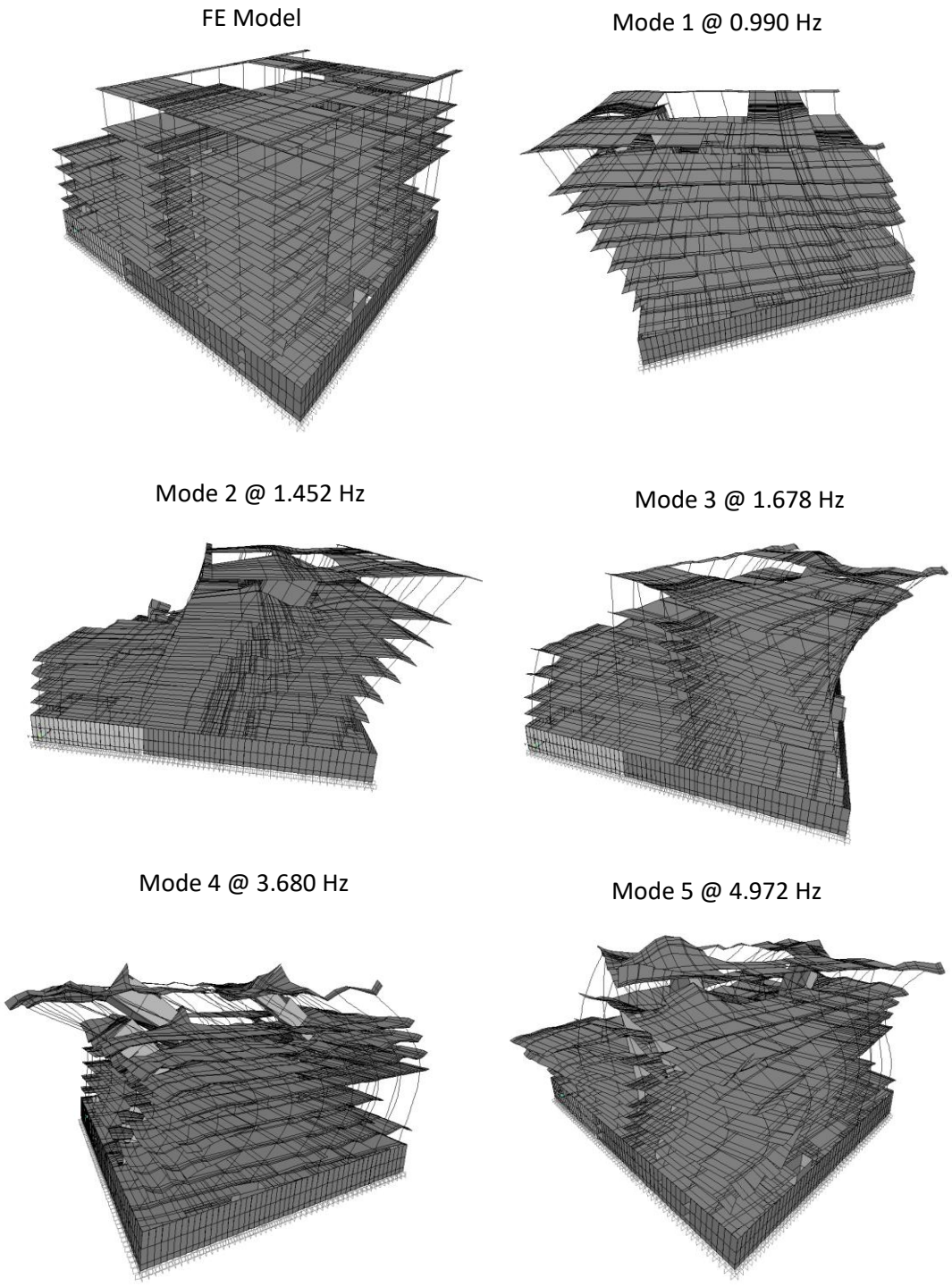

Fig. 4 FE model 1 and typical animated shapes of first five vibration modes

4 Model Calibration and Validation

After developing an initial physics-based FE model and identifying the dynamic characteristics by experimental evaluations of the actual structure, the next step is to calibrate and validate the physics-based model in a manner to suit the objectives of the St-Id application. Hence, the calibration step is one of the most important tasks of St-Id of a structure. In this study, the sensitivity based automated model calibration process is implemented through FEMtools software package [26].

4.1 Response Selection, Parameter Selection and Sensitivity Analysis

A successful model calibration depends on appropriate selection of uncertain parameters; hence careful attention should be paid on choosing uncertain parameters in the FE model to increase the physical relevance of the parameters in the updated model. Also, it is important that all the chosen parameters are sensitive to the selected responses. Nevertheless, for large structures selection of parameters that can be systematically coped will facilitate automated model calibration.

In this study, the chosen uncertain parameters are as follows.

- Young's Modulus (E)
- Mass Density (ρ)
- Cross Sectional Area (AX)
- Torsional Stiffness (IX)
- 2nd Moment of Area about Y (IY)
- 2nd Moment of Area about Z (IZ)
- Shell Thickness (H)

Their detailed distributions are tabulated in Table 3~~Table 3~~.

Table 3 Description of model parameters used in sensitivity analysis

Uncertain parameter	Element types	Number of finite elements
E	All elements	9400
ρ	All elements	9400
AX	Frames (Columns)	1400
IX	Frames (Columns)	1400
IY	Frames (Columns)	1400
IZ	Frames (Columns)	1400
H	Shells (Floor Slabs only)	5680
		30080 (Total)

Since the parameters chosen are of different types, relative sensitivities were used for the sensitivity analysis (the sensitivity matrix was obtained by finite difference method).

$$[S_r] = \left[\frac{\delta R_j}{\delta P_j}\right][P_j] \tag{2}$$

$[S_r]$ = Relative sensitivity matrix;

$[P_j]$ = A diagonal, square matrix holding parameter values

Then the relative sensitivities were normalized with respect to the response values.

$$[S_n] = [S_r][R_i]^{-1} = [R_i]^{-1}\left[\frac{\delta R_j}{\delta P_j}\right][P_j] \tag{3}$$

$[S_n]$ = Normalized relative sensitivity matrix;

$[R_i]$ = A diagonal, square matrix holding the response values

Thorough investigations were carried out to identify the relationship of parameter changes of the local elements to each response. As an example, Fig. 5~~Fig. 5~~ and Fig. 6~~Fig. 6~~ show the normalized sensitivities of ~~the~~ parameters ~~for the~~ against two responses, i.e. frequency and MAC of mode number 1.

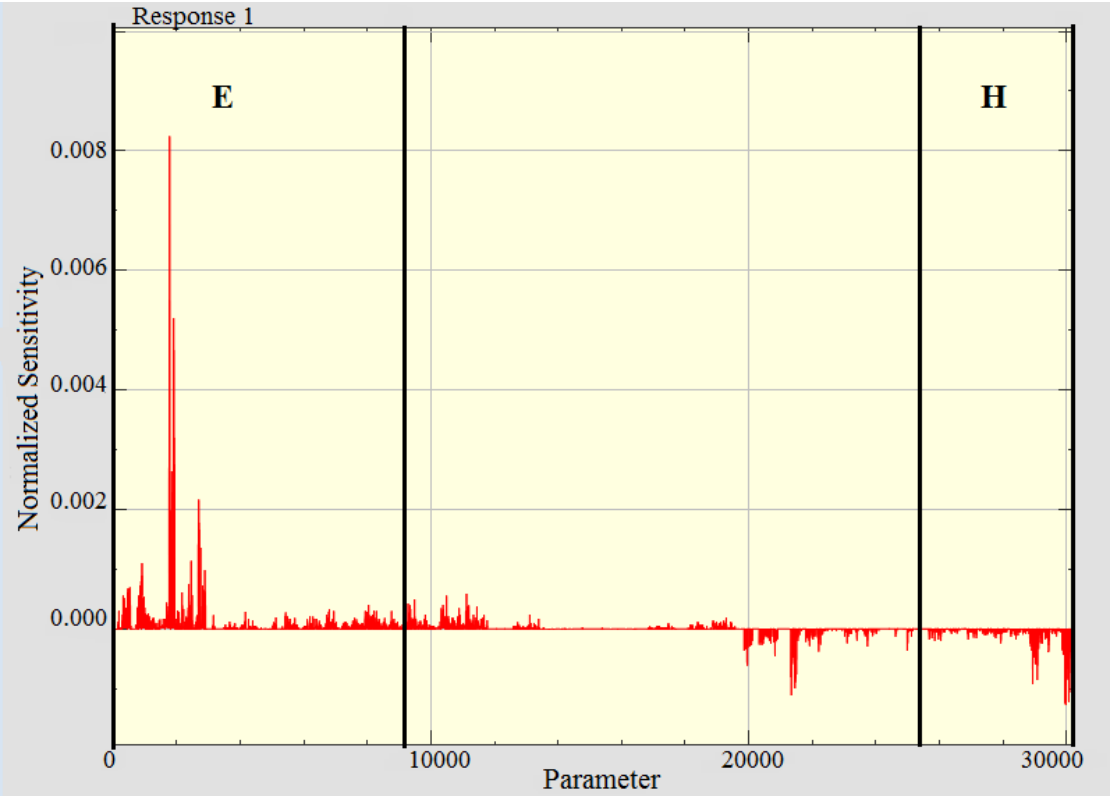

Fig. 5 Normalized sensitivity ~~versus~~ of parameter ~~for the~~against frequency of mode 1

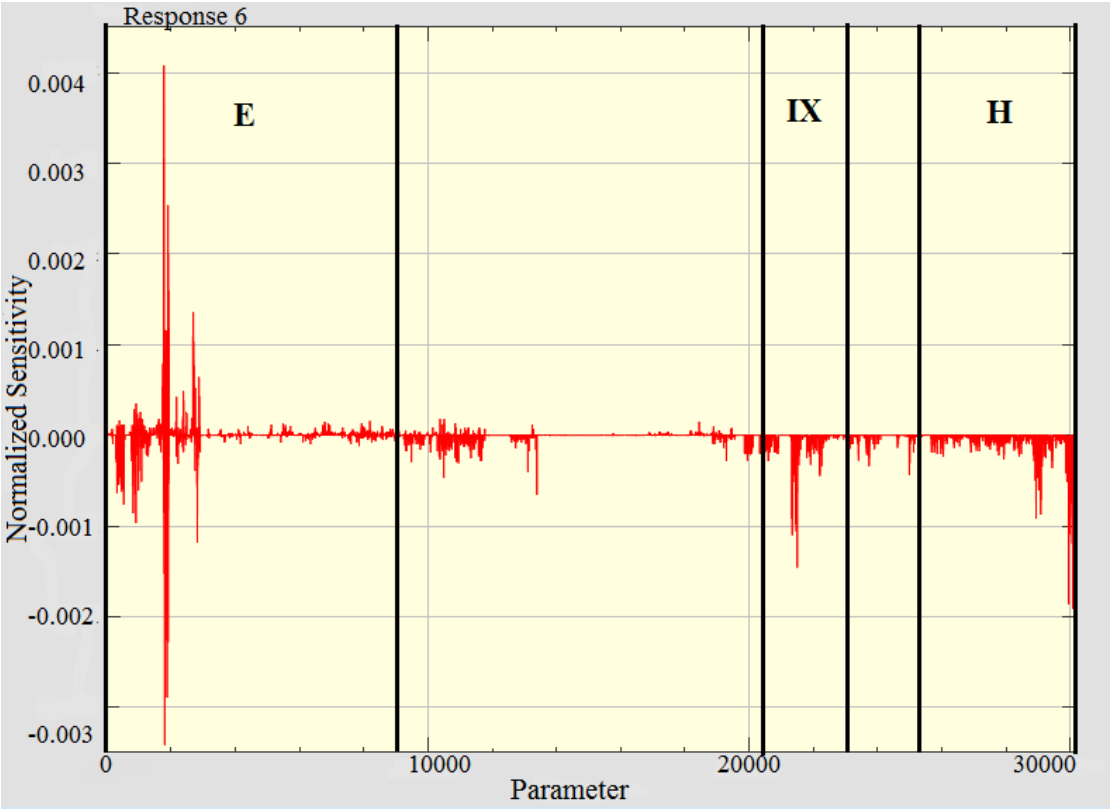

Fig. 6 Normalized sensitivity ~~versus~~ of parameter ~~for the~~ against MAC of mode 1

These figures show that the parameters E and H for some local elements have significant sensitivity for both responses selected (1 & 6). Similarly, this process is carried out for all the ten responses to identify the sensitivity of the chosen parameters for each response. Based on the analysis the parameters with high sensitivities were identified as tabulated in Table 4~~Table 4~~.

Table 4 High sensitive parameters and correlation nature for the selected responses

Response No	Response Description	High sensitive parameters & correlation nature
1	Mode 01 – Frequency	E – Positive Correlation H – Positive Correlation
2	Mode 02 – Frequency	E – Positive Correlation RHO – Negative Correlation H – Positive Correlation
3	Mode 03 – Frequency	E – Positive Correlation AX – Positive Correlation RHO – Negative Correlation H – Positive Correlation
4	Mode 04 – Frequency	E – Positive Correlation IY – Positive Correlation IZ – Positive Correlation H – Positive Correlation
5	Mode 05 – Frequency	E – Positive Correlation IY – Negative Correlation IZ – Negative Correlation H – Positive Correlation
6, 7, 8, 9, 10	Mode 01, 02, 03, 04, 05 – Mode Shape	E – Positive Correlation IX – Positive/Negative Correlation AX – Positive/Negative Correlation H – Positive/Negative Correlation

Hence, based on the sensitivity analysis results, sensitive local elements for each response were identified and selected for model calibration. For most of the tuning parameters, groups were defined for the identified elements based on element type to make the updated parameters physically realisable and meaningful. One notable exception was no sets were used for the shell thickness. As mentioned earlier, average slab thicknesses were used in the FE model and the internal variation was high in the actual structure. Hence, it is justifiable to exclude slab thicknesses in the parameter set.

4.2 Model Calibration and Parametric Study

After selection of responses and appropriate parameters, model calibration was carried out. Sensitivity based parameter estimation coupled with pseudo-inverse parameter estimation was used as the calibration algorithm.

The Taylor series expansion limited to linear terms was used to express the relationship between the modal characteristics and the structural parameters.

$$\{R_e\} = C + [S](\{P_u\} - \{P_0\}) \tag{4}$$

$$\{\Delta R\} = [S]\{\Delta P\} \tag{5}$$

$\{R_e\}$ = Experimental data

$\{R_a\}$ = Predicted responses for a given state $\{P_0\}$ of the parameter values

$\{P_u\}$ = Updated parameter values

To determine the desired parameter variation pseudo-inverse of the sensitivity matrix was used since the number of parameters was lower than the number of equations.

$$\{\Delta P\} = ([S]^t[S])^{-1}[S]^t\{\Delta R\} \tag{6}$$

The least squares solutions obtained from the above equation minimize the residue:

$$\{residue\} = [S]\{\Delta P\} - \{\Delta R\} \tag{7}$$

The calibration process would be stopped when a given residue value was achieved, or a given minimum improvement between two consecutive iterations was achieved or maximum number of iterations achieved. For this particular case study, these values were set as follows;

- Minimum residue value - 0.1%
- Minimum improvement between two consecutive iterations - 0.01%
- Maximum number of iterations - 100

For the model calibration, maximum and minimum limits were implemented to make the changes physically realisable and meaningful. Initially, 15% upper and lower bounds were implemented for all the selected parameters and the calibration process stopped after 33 iterations (due to the minimum improvement between two consecutive improvements falls below the established value of 0.01%). Comparisons of frequencies and MAC values before and after model calibration are summarized in Table 5~~Table 5~~ and Table 6~~Table 6~~ respectively. Although some improvement in frequencies can be found in Table 5~~Table 5~~, there is a significant drop in the MAC values of mode shape pairs 4 and 5 (Table 6~~Table 6~~).

Table 5 Comparison of frequencies before and after model calibration with 15% parameter change bounds scenario

Mode Number	$Freq^{OMA}$ (Hz)	Before calibration		After calibration	
		$Freq^{FEM}$	$Error^{FEM-OMA}$	$Freq^{FEM}$	$Error^{FEM-OMA}$
1	1.147 Hz	0.990 Hz	-13.69%	1.041 Hz	-9.24%
2	1.544 Hz	1.452 Hz	-5.96%	1.526 Hz	-1.17%
3	1.653 Hz	1.678 Hz	1.51%	1.705 Hz	3.15%
4	3.989 Hz	3.680 Hz	-7.75%	3.835 Hz	-3.86%
5	4.254 Hz	4.972 Hz	16.88%	3.889 Hz	-8.58%

Table 6 Comparison of MAC values before and after model calibration with 15% parameter change bounds scenario

Mode Shape Pair	Before calibration	After calibration
1	89.9%	89.0%
2	50.5%	67.2%
3	42.5%	50.9%
4	63.2%	36.6%
5	68.4%	34.7%

Since such MAC values would not be considered as acceptable, a parametric study was then introduced to find the optimum level of allowable parameter change to improve the results of the updated FE model. Here the shell thickness was chosen as the parameter for the parametric study, because not only it was sensitive to all the responses but also it had the highest sensitivity for all the selected responses (see Table 4~~Table 4~~). In the parametric study, upper and lower bounds of all the responses except shell thickness (H) were kept at 15%. For the shell thickness, upper and lower bounds were changed from 15% - 45% with an interval of 7.5%. Fig. 7~~Fig. 7~~ illustrates the relationship between error in frequency (against OMA frequency) and the change in upper and lower bounds for shell thickness. On the other hand, Fig. 8~~Fig. 8~~ shows the variation of MAC value for each mode shape with the change in upper and lower bounds of the shell thickness.

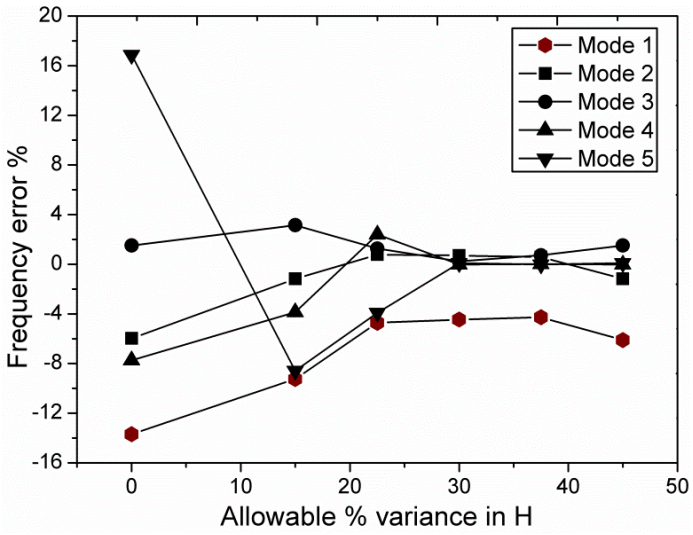

Fig. 7 Frequency error versus allowable variance in shell thickness

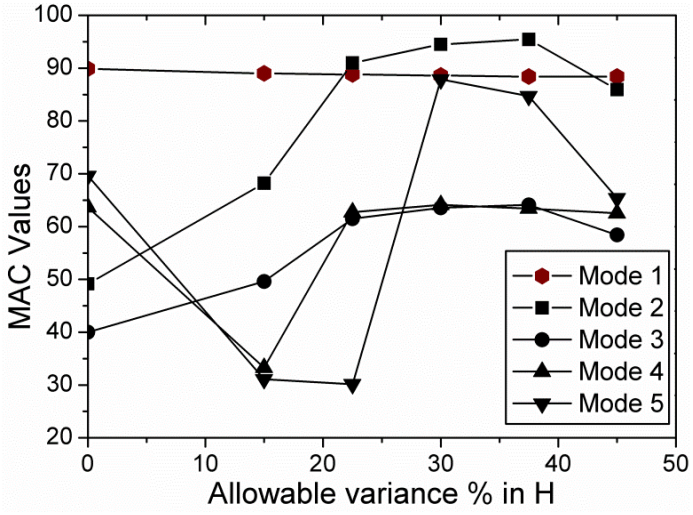

Fig. 8 MAC value versus allowable variance in shell thickness

The frequency error for all the modes becomes minimum when the allowable variance in shell thickness is 30% (Fig. 7~~Fig. 7~~). Also, the MAC values of almost all the mode shape pairs reach highest value at the same allowable variance in shell thickness (Fig. 8~~Fig. 8~~). Hence, this scenario was chosen as the final configuration to perform the model calibration process. Table 6 summarises the maximum parameter changes for this configuration. The maximum allowable upper and lower bound limits were achieved by four parameters, namely E (15%), Mass Density (15%), IY (15%) and H (30%). The minimum variance was achieved by IX which was the least sensitive parameter for all the responses.

Table 7 Maximum parameter change with the final calibration configuration

Parameter	Initial Value	Max. Value	Max. Change	Min. Value	Min. Change
E	3.5E+07 kN/m^3	4.26E+07 kN/m^3	+15 %	2.98E+07 kN/m^3	-15 %
RHO	2.4 kN/m^3	2.76 kN/m^3	+15 %	2.04 kN/m^3	-15 %
AX	Varies	Varies	+8.34 %	Varies	-9.61 %
IX	Varies	Varies	+1.31 %	Varies	-1.51 %
IY	Varies	Varies	+14.3 %	Varies	-15 %
IZ	Varies	Varies	+10.7 %	Varies	-4.35 %
H	Varies	Varies	+30 %	Varies	-30 %

Results after 39 iterations for the final calibration configuration are summarized in Table 8~~Table 8~~. The table shows the OMA frequencies and the FE model frequencies for both before and after model calibration for the first five modes. From Table 8~~Table 8~~, it can be seen that four out of five modes of the calibrated FE model are in excellent match with the corresponding OMA modes with only 1.3% or less error. The largest error of 4.6% is with the first mode which still shows a very good numerical-experimental correlation for practical modelling purposes especially when considering the low frequency characteristic of this particularly mode as well as the scale of this building structure.

Table 8 Comparison of frequencies before and after model calibration with the final calibration configuration

Mode Number	Freq ^{OMA} (Hz)	Before calibration		After calibration	
		Freq ^{FEM}	Error $^{FEM-OMA}$	Freq ^{FEM}	Error $^{FEM-OMA}$
1	1.147 Hz	0.990 Hz	-13.69%	1.096 Hz	-4.62%
2	1.544 Hz	1.452 Hz	-5.96%	1.555 Hz	0.71%
3	1.653 Hz	1.678 Hz	1.51%	1.657 Hz	0.24%
4	3.989 Hz	3.680 Hz	-7.75%	3.988 Hz	-0.03%
5	4.254 Hz	4.972 Hz	16.88%	4.258 Hz	0.09%

Table 9~~Table 9~~ shows the MAC value for each mode shape pair before and after calibrating the model. A graphical comparison of mode shapes of the FE model and OMA is shown in Figure 10. From Table 9~~Table 9~~, there are three pairs matching with 84% or higher MAC values. The other two modes also have a reasonable match with over 60% MAC values. This can be considered as an acceptable result considering the complexities of the structural details and boundary conditions as previously mentioned as well as the demanding ambient monitoring conditions. In fact, it has been widely acknowledged that precise mode shape measurements are very difficult to be obtained under ambient testing circumstances, see for instance [27]

Table 9 Comparison of MAC values before and after model calibration with the final calibration configuration

Mode Shape Pair	Before calibration	After calibration
1	89.9%	88.6%
2	50.5%	90.2%
3	42.5%	63.1%

4	63.2%	63.3%
5	68.4%	84.4%

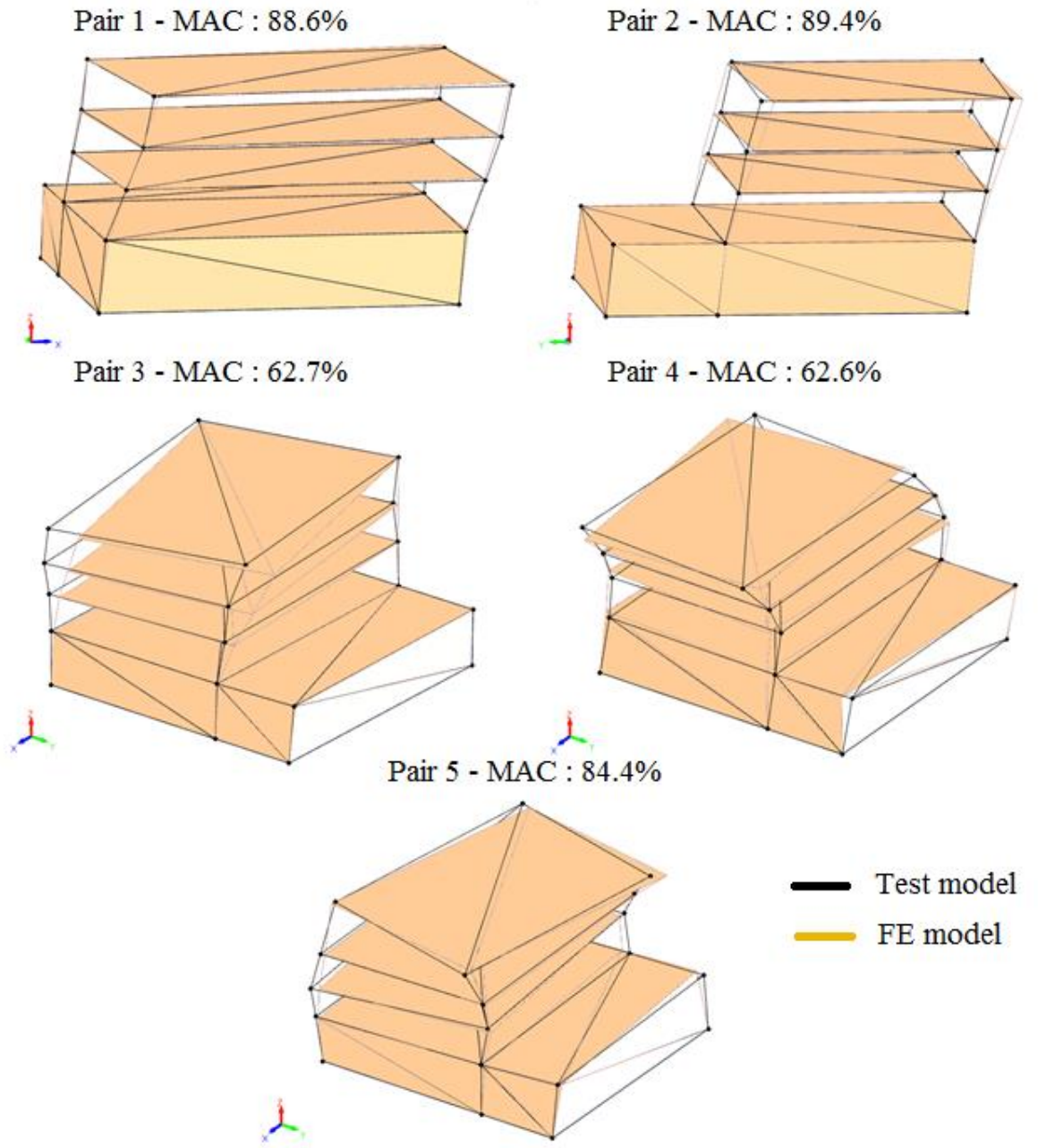

Fig. 9 Graphical comparison of mode shapes between calibrated FE model and OMA results

To highlight the efficacy of the St-Id procedure adopted in this research, it is worth comparing the results of this study with the results of similar cases reported in literature. As mentioned in section 1, Ventura et al. [21] conducted an automated model updating on a 15 story building updating initial FE model developed based on design drawings by first six vibration modes

derived by OMA. The largest error in terms of frequency and maximum MAC value for the mode shape pairs is 13.3% and 85% respectively as opposed to the 4.6% and 89.4% in this case study. Further, in the aforementioned case study most tuning parameters were subjected to higher variation from the initial values such as E values of floor slabs 70% and I values of columns 50% which tend to cause the loss in physical relevance of the updated FE models. In the study herein, most parameter variations were limited to 15% (except the shell thickness of the slabs with 30% variation bounds) to ensure that the updated FE model was physically relevant and meaningful.

5 Conclusion

This paper presented a comprehensive St-Id study on a benchmark medium-rise building with a focus on strategies to obtain appropriate initial analytical model as well as to manage tuning parameters effectively to maximise the model-test correlation while maintaining the physical relevance of the outcome. From the results of this research, the following conclusions and recommendations can be drawn for enabling effective St-Id processes for medium-rise buildings

- Initial analytical models should be constructed based on as-built drawings and other as-constructed documents rather than design drawings to account for changes occurred during the construction process.
- Compared to high-rise buildings, boundary conditions of medium-rise buildings especially those that have basements tend to have more significant impact on the initial analytical model. Hence, different modelling options for boundary components should be carefully evaluated against each other as well as against experimental results.

- The use of average thickness for shell elements of floor slab systems in the initial model speeds up the modelling process since thickness variations are normally high in medium-rise buildings especially those that are used as multi-purpose facilities.
- Since the number of tuning parameters in real building structures is often very large, the exclusion of low-sensitivity parameters is a must to avoid ill condition of the model calibration process. This can be realised by examining the relationship between parameter changes and the main responses such as the modal data of the first few modes.
- The use of parameter set and appropriate parameter bounds should be used to ensure the calibrated model is physically relevant and meaningful. High-impact parameters with high and arbitrary variations like the thickness of floor finite elements should have larger variation bounds and can be excluded from parameter set to allow their calibration to be treated in a more detailed manner. The use of sensitivity analysis is also recommended for determining optimal range of variation bounds for these types of parameters.

6 Acknowledgement and conflict of interest declaration

The data used in this research is from the PhD research of the second author between 2014 and 2017 at QUT. The study was funded by Queensland University of Technology PhD Scholarships and in part by the Australian Research Council Discovery Project No. DP160101764. The authors declare they have no conflict of interest.

7 References

1. Aktan, A.E. and J.M.W. Brownjohn, *Structural identification: Opportunities and challenges.* Journal of Structural Engineering (United States), 2013. **139**(10): p. 1639-1647.
2. Aktan, E., et al., *Structural identification: Analytical aspects.* Journal of structural engineering New York, N.Y., 1998. **124**(7): p. 817-829.
3. Catbas, F.N., et al., *Limitations in structural identification of large constructed structures.* Journal of Structural Engineering, 2007. **133**(8): p. 1051-1066.

4. Beck, J.L. and P.C. Jennings, *Structural identification using linear models and earthquake records.* Earthquake Engineering & Structural Dynamics, 1980. **8**(2): p. 145-160.
5. Hudson, D.E., *Dynamic tests of full-scale structures.* 1977. **103**(6): p. 1141-1157.
6. Yao, J.T.P., *Damage assessment and reliability evaluation of existing structures.* Engineering Structures, 1979. **1**(5): p. 245-251.
7. Aktan, A.E., et al., *Structural identification for condition assessment: experimental arts.* Journal of structural engineering New York, N.Y., 1997. **123**(12): p. 1674-1685.
8. Aoki, T. and D. Sabia, *Structural identification and seismic performance of brick chimneys, Tokoname, Japan.* Structural Engineering and Mechanics, 2005. **21**(5): p. 553-570.
9. Bonato, P., R. Ceravolo, and A. De Stefano, *The use of wind excitation in structural identification.* Journal of Wind Engineering and Industrial Aerodynamics, 1998. **74-76**: p. 709-718.
10. Chan, T.H.T., et al., *Concurrent multi-scale modeling of civil infrastructures for analyses on structural deteriorating-Part II: Model updating and verification.* Finite Elements in Analysis and Design, 2009. **45**(11): p. 795-805.
11. Liu, H., Z. Yang, and M.S. Gaulke, *Structural identification and finite element modeling of a 14-story office building using recorded data.* Engineering Structures, 2005. **27**(3): p. 463-473.
12. Jaishi, B. and W.-X. Ren, *Structural finite element model updating using ambient vibration test results.* Journal of Structural Engineering, 2005. **131**(4): p. 617-628.
13. Zivanovic, S., A. Pavic, and P. Reynolds, *Finite element modelling and updating of a lively footbridge: The complete process.* Journal of Sound and Vibration, 2007. **301**(1-2): p. 126-145.
14. Brownjohn, J.M.W. and P.-Q. Xia, *Dynamic assessment of curved cable-stayed bridge by model updating.* Journal of structural engineering New York, N.Y., 2000. **126**(2): p. 252-260.
15. Zhang, Q.W., T.Y.P. Chang, and C.C. Chang, *Finite-element model updating for the Kap Shui Mun cable-stayed bridge.* Journal of Bridge Engineering, 2001. **6**(4): p. 285-294.
16. Cismasiu, C., A.C. Narciso, and F.P. Amarante Dos Santos, *Experimental Dynamic Characterization and Finite-Element Updating of a Footbridge Structure.* Journal of Performance of Constructed Facilities, 2015. **29**(4).
17. Daniell, W.E. and J.H.G. Macdonald, *Improved finite element modelling of a cable-stayed bridge through systematic manual tuning.* Engineering Structures, 2007. **29**(3): p. 358-371.
18. Ding, Y. and A. Li, *Finite element model updating for the Runyang Cable-stayed Bridge tower using ambient vibration test results.* Advances in Structural Engineering, 2008. **11**(3): p. 323-335.
19. Fei, Q.G., et al., *Structural health monitoring oriented finite element model of Tsing Ma bridge tower.* International Journal of Structural Stability and Dynamics, 2007. **7**(4): p. 647-668.
20. Wu, J.R. and Q.S. Li, *Finite element model updating for a high-rise structure based on ambient vibration measurements.* Engineering Structures, 2004. **26**(7): p. 979-990.
21. Ventura, C., et al. *FEM updating of tall buildings using ambient vibration data*. in *Proceedings of the sixth European conference on structural dynamics (EURODYN)*. 2005.
22. Green Building Council Australia. *QUT Science and Engineering Centre: 5 Star Green Star Rating - Green Star - Education Design v1*. 2011; Available from: http://www.gbca.org.au/project-profile.asp?projectID=944 (accessed July, 2017).
23. Nguyen, T., et al., *Development of a cost-effective and flexible vibration DAQ system for long-term continuous structural health monitoring.* Mechanical Systems and Signal Processing, 2015. **64-65**: p. 313-324.
24. Nguyen, T., *SHM through flexible vibration sensing technologies and robust safety evaluation paradigm*, 2014, Queensland University of Technology.
25. Nguyen, T., T.H.T. Chan, and D.P. Thambiratnam, *Field validation of controlled Monte Carlo data generation for statistical damage identification employing Mahalanobis squared distance.* Structural Health Monitoring, 2014. **13**(4): p. 473-488.

26. Dynamic design solutions, *FEMtools Model Updating User's Guide (Version 3.8)*, 2015, Dynamic Design Solutions NV (DDS), Leuven, Belgium.
27. Friswell, M.I., *Damage identification using inverse methods.* Philosophical Transactions of the Royal Society of London A: Mathematical, Physical and Engineering Sciences, 2007. **365**(1851): p. 393-410.